Low-Cost and Accurate Broadband Beamforming Based on Narrowband Sub-Arrays

Abdullah Alshammary and Stephan Weiss
Department of Electronic & Electrical Engineering, University of Strathclyde, Glasgow G1 1XW, Scotland
Email: {abdullah.alshammary, stephan.weiss}@strath.ac.uk

***Abstract*—Simplified broadband beamformers can be constructed by sharing a single tapped-delay-line within a narrowband subarray. This paper discusses the use of fractional delay filters to a steering in the digital domain. For the narrowband subarrays, an optimisation approach is proposed to maintain an off-broadside look direction constraint as best as possible across a given frequency range. We demonstrate the advantage that this approach has for generating beamformers with accurate off-broadside look direction compared to a benchmark.**

I. Introduction

Antenna array has been widely studied and utilised in narrowband signal transmission and detection. However many arrays will be required to operate over a wider bandwidth in order to enhance performance. In radar for example, the use of wideband waveforms increases range resolution and reduces peak power. In communication, wideband transmission can yield a higher information rate.

While theoretical broadband beamforming requires each array element to be followed by a tap-delay-line (TDL) implementing frequency-selective filters [1], for most radar applications this is not practical: attaching a time delay module or TDL behind each array element is currently impossible due to small sensor spacing and limited weight, space and power. Instead however, elements can be grouped into smaller areas within the array apertures called subarrays. A compromise for broadband processing in state-of-the-art broadband radar hardware is therefore to operate complex multipliers following the sensor elements. The subarray outputs are then fed into hardware time delay units in order to reach an acceptable performance across the operating bandwidth [2].

The architecture of narrowband subarrays followed by a time delay is referred to as a subarray structure, and has been addressed e.g. in [3], [4], [5], [6]. The general problem that has been researched is the tiling of the subarrays in order to minimize quantization sidelobes [3], [4], [5]. Sometimes also the narrowband beamforming weights are optimized in order to suppress sidelobes in the beamformer's broadband response [3], [7].

This paper explores a digital implementation of time delay using fractional delay filters, and instead of optimizing sidelobe levels, in the first instance we are concerned with minimizing the deviation in the beamformer's gain in look-direction. We demonstrate that the combination of fractional delay filters and optimization of narrowband weight can provide an acceptable performance.

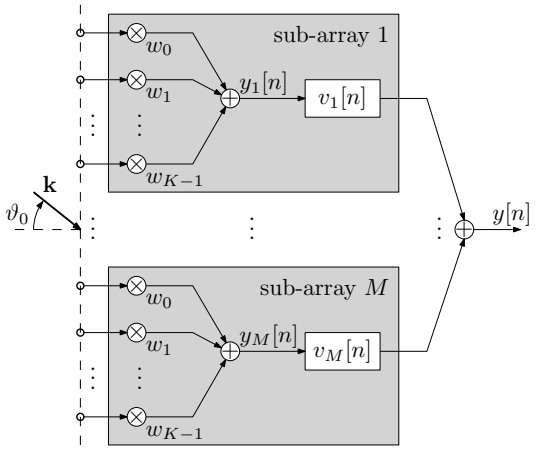

Fig. 1. Uniform linear array divided into M narrowband sub-arrays of K sensors each, which are then combined via M filters $v_m[n]$, $m = 1 \dots M$. The angle of arrival ϑ_0 of an incoming farfield waveform with slowness vector $\mathbf{k}/c$ is measured against broadside.

The paper is organised a follows. The subarray architecture is defined in Sec. II, with its tap delay line filters constructed as fractional delay filters in Sec. III. Sec. III reviews the standard construction of the narrowband beamformers by means of designing for the centre frequency point if operation over a wider badnwidth is desired. This beamformer design is optimised in Sec. IV and demonstrated in Sec. V. Finally, conclusions are drawn in Sec. VI.

II. Array Configuration

The subarray configuration addressed in this paper is shown in Fig. 1, where M patches each contain a subarray of K elements. he kth array element is positioned at $\mathbf{r}_k = \frac{1}{cT_s}[x_k\ y_k\ z_k]^{\mathrm{T}}$ in 3-dimensional Cartesian space with coordinates x_k, y_k and z_k, propagation speed c and sampling period T_{s}. If a wavefront arrives from an elevation ϑ and azimuth φ, then the delay at the kth sensor relative to the coordinate system's origin is $\tau_k = \mathbf{k}_{\vartheta,\varphi}^{\mathrm{T}}\mathbf{r}_k$, where $\mathbf{k}_{\vartheta,\varphi}$ is a unit vector normal to the planar wavefront,

$$\mathbf{k}(\theta,\phi) = \begin{bmatrix} \sin\theta\cos\phi \\ \sin\theta\sin\phi \\ \cos\theta \end{bmatrix} . \tag{1}$$

If normalised by the propagation speed c, $\mathbf{k}_{\vartheta,\varphi}/c$ is also known as the source's slowness vector. For simplificity, our

analysis below will rely on a uniform linear array as shown in Fig. 1 containing MK sensors organized into M subarrays comprising K elements each. The element spacing is $d = 1/(2cT_\mathrm{s})$.

Subarray elements are followed by complex weights w_k capable of performing narrowband beamforming. If the M patches are identically configured, then these weights are identical cross the M subarrays, and can be organised into a $\mathbf{w}$ as

$$\mathbf{w}^\mathrm{H} = \left[\begin{array}{cccc} w_1 & w_2 & \ldots & w_K \end{array} \right] \quad . \tag{2}$$

As shown in Fig. 1, each subarray then feeds into on of M tap delay lines with coefficients $v_m[n]$, where n is the discrete time index. The purpose of this tap delay line processor is to coarsely allign the subarray centre points with respect to each other. Thereafter, the coefficients $\mathbf{w}$ fine-tune the response, but using the capabilities of a narrowband beamformer which generally can only be accurate at one specific frequency.

The aim of this paper is firstly to adjust the tap delay filters and secondly to optimise the narrowband coefficient over the operating frequency range in order to obtain a beamforming response with a constraint in a particular look direction.

III. Broadband Subarray Design

This section details the adjustment of the subarray tap delay line filters in Sec. III-A, and highlights some of the problems in adjusting the narrowband beamformers $\mathbf{w}$ in order to achieve a broadband response in Sec. III-B

A. Fractional Delay Filters

To coarsely align the different subarrays for an incoming waveform, the time delay with which the wavefront impinges on the array must be compensated explicitly. Since these delays are generally not integer multiples of the sampling period T_s, fractional delay filters are required.

To approximate a fractional delay, a number of different filter implementations have been proposed [8]. While the optimum fractional delay is a sinc function of infinite support, finite causal version require a truncation with a rectangular window $p_N[n] = \sum_{\nu=-N}^{N} \delta[n-\nu]$ and a time shift. Such filters generally are inaccurate particularly close to half of the sampling rate, but performance can be enhanced by tapered windows [9], [10]. Using e.g. a von Hann window

$$w[n] = \sin^2(\frac{\pi n}{2N}) p_{2N}[n] \; , \tag{3}$$

where the sine function tapers a rectangular window

$$p_{2N} = \left\{ \begin{array}{ll} 1 & 0 \leq n \leq 2N \\ 0 & \text{otherwise} \; , \end{array} \right. \tag{4}$$

a filter implementing a fractional delay τ_m can be constructed as

$$v_m[n] = \mathrm{sinc}[n - N - \tau_m] \cdot w[n - N - \tau_m] \tag{5}$$

where $\mathrm{sinc}[n]$ is the sinc function and τ the fractional delay.

As a demonstration of the accuracy, the sinc and von Hann-windowed sinc filters for the case $N = 16$ are depicted in Fig. 2(a) for $\tau = \frac{1}{2}$. To create a causal design, the fractional

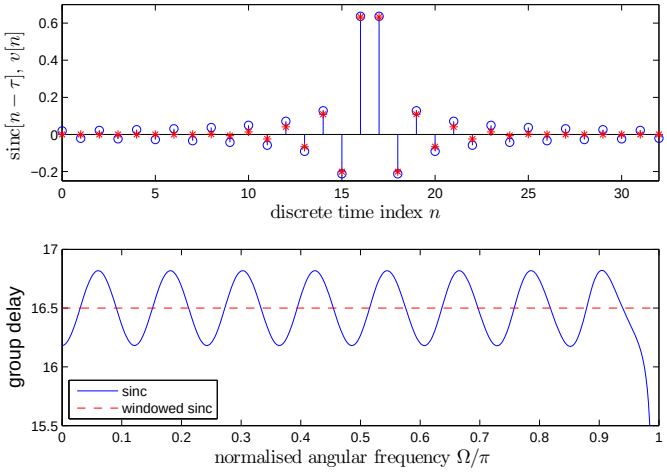

Fig. 2. (a) Impulse responses and (b) group delays for fractional delay filters constructed from sinc and windowed sinc functions for $N = 16$ and $\tau = 16.5$.

delay is approximately centred in the filter, such that in fact $\tau = N + \frac{1}{2}$. The group delays for the two systems in Fig 2(b) show the variability of the rectangularly-windowed sinc, while the tapered window design exhibits a much better phase behaviour and closely matches τ with its group delay over the operating frequency range.

With the above design of (5), the subarrays can be aligned coarsely with respect to their centre point. If $\mathbf{r}_m$ is the centre point of the mth subarray, then $\tau_m = \mathbf{k}^\mathrm{T}\mathbf{r}_m$, with $\mathbf{k}/c$ the slowness vector of the incoming waveform.

B. Narrowband Array Response

In this section we will analyse the look direction of a narrowband subarray beamformer $\mathbf{w}$ when operated across a wider bandwidth. For this purpose, we define a steering vector $\mathbf{a}$ that characterises the phase profile of an incoming waveform with slowness vector $\mathbf{k}/c$,

$$\mathbf{a}(\Omega, \vartheta) = \frac{1}{\sqrt{K}} \left[\begin{array}{c} e^{j\Omega\tau_1} \\ e^{j\Omega\tau_2} \\ \vdots \\ e^{j\Omega\tau_K} \end{array} \right] \tag{6}$$

where Ω is specified normalised angular operating frequency, and $\tau_k = \mathbf{k}^\mathrm{H}\mathbf{r}_k$ the delay experienced at the kth array element positioned at location $\mathbf{r}_k$ relative to the origin. The dependency of the l.h.s. term on ϑ is given through the slowness vector defined in (1), and will be generally omitted below.

Using the steering vector definition above, we want to design a subarray beamformer $\mathbf{w}$ and see how its reference frequency influences the look direction when the overall beamformer is operated over a wider frequency range. If the gain in look direction ϑ_0 is expected to be unity, then a frequency-dependent error

$$e_1(\Omega) = \mathbf{a}^\mathrm{H}(\Omega)\mathbf{w} - 1 \tag{7}$$

can be evaluated over a range of frequencies $\Omega \in [\Omega_l; \Omega_u]$, leading to an overall cost function

$$\xi_1 = \frac{1}{2\pi} \int_{\Omega_l}^{\Omega_u} |e_1(\Omega)|^2 d\Omega \; . \tag{8}$$

Here, Ω_l and Ω_u are the lower and upper frequency bounds of the operating range, respectively. A second error can be defined by neglecting the phase in look direction and only measuring the error in magnitude, i.e.

$$e_2(\Omega) = |\mathbf{a}^{\mathrm{H}}(\Omega)\mathbf{w}| - 1 \; , \tag{9}$$

with an overall cost ξ_2 function across the operating range defined analogous to (8).

Array weights obtained from delay and sum beamformers have been suggested for broadband subarrays [11], [12], [6] using a Wiener-Hopf type solution [13], [14],

$$\mathbf{w}_0 = (\mathbf{a}(\Omega_0)\mathbf{a}^{\mathrm{H}}(\Omega_0))^{-1}\mathbf{a}(\Omega_0)\underline{1} \; . \tag{10}$$

Wiener-Hopf is simply the pseudo-inverse of the steering vector at the specified frequency and look direction. Assuming a unity constraint in look direction, the pseudo-inverse folds back to delay and sum solution, such that

$$\mathbf{w}_0 = \mathbf{a}(\Omega_0) \; . \tag{11}$$

Typically the median frequency of the frequency band $\Omega_0 = \frac{\Omega_u + \Omega_l}{2}$ serves as a suitable reference point to synthesis the pattern and frequency response, as suggest e.g. in [1] [11, p. 31]and [15].

In the following we will estimate the total error ξ_1 in look direction as a result of designing the array weights at center frequency. Evaluating the cost function ξ_1 with a narrowband beamformer designed for frequency Ω_0, ξ_1 can be evaluated analytically and shown to yield

$$\begin{aligned}\xi_1 =& \frac{1}{2\pi K^2} \sum_{n=1}^{K} \sum_{m=1}^{K} \frac{1}{-j(\tau_n + \tau_m)} \cdot \\ & \cdot \left(e^{-j(\Omega_u - \Omega_0)(\tau_n + \tau_m)} - e^{-j(\Omega_l - \Omega_0)(\tau_n + \tau_m)}\right)] \\ & + \frac{1}{2\pi K} \sum_{n=1}^{K} [\frac{2}{j\tau_n}(e^{-j(\Omega_u - \Omega_0)\tau_n} - e^{-j(\Omega_l - \Omega_0)\tau_n})] \\ & + \frac{\Delta\Omega}{2\pi} \; ,\end{aligned} \tag{12}$$

where $\Delta\Omega = \Omega_u - \Omega_l$ is the desired bandwidth.

Figure 3 show the cost function described in equation (12) for different angles of arrival ϑ_0 and reference frequencies Ω_0. Notice that in Figure 3 choosing the median frequency as a reference point approximately corresponds to minimum total error for angles of arrival up to $\sin(\vartheta_0) = .4$ or $\vartheta_0 = 23.6°$. Beyond that, the total error varies sinusoidally causing multiple peaks.

To emphasise that selecting Ω_0 as the centre frequency will not generally minimise ξ_1 and ξ_2, Fig. 4 depicts the two cost functions for the case $K = 32$ and $\vartheta = 60°$, with $\Omega_l = \frac{\pi}{2}$ and $\Omega_u = \pi$. For both cost functions, the minima

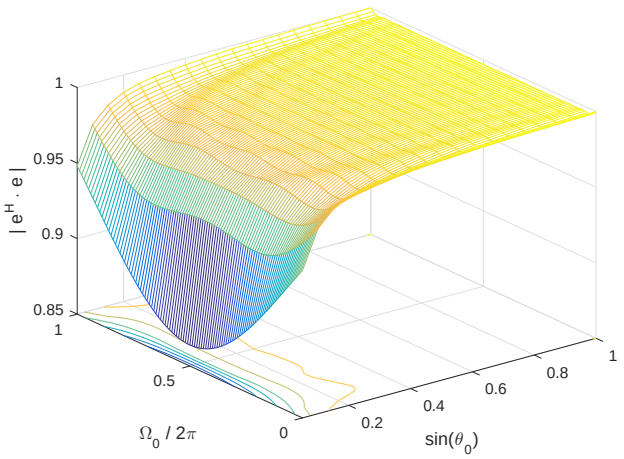

Fig. 3. Cost function ξ_1 as defined in (12) for a $K = 32$ elements uniform linear array.

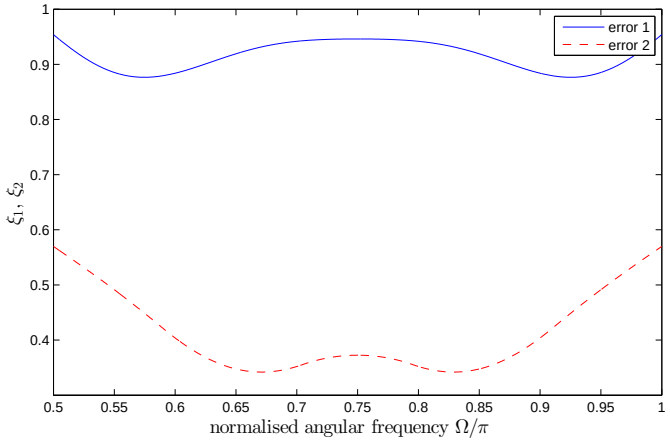

Fig. 4. cost function from equation 12 for 32 elements uniform linear array with $\beta = 0.01$.

appear away from the centre. Therefore, designing the subarray broadband beamformer via the centre frequency will generally not optimise the response. Therefore, the next section will propose a different optimisation approach.

IV. Proposed Broadband Subarray Design

The analysis in the previous section indicated that designing the subarray weights at the median frequency do not always lead to the lowest response error in look direction. Therefore, this section will optimise the coefficient set $\mathbf{w}$ and remove the constraint that the coefficients only apply a phase shift: instead, the magnitude can also be adjusted such that $\mathbf{w} \in \mathbb{C}^K$.

Given that $\mathbf{a}(\Omega, \vartheta_0)$ is the steering vector in look direction ϑ_0 at a normalised angular frequency Ω. Then deviation from unit gain by a beamformer with weights $\mathbf{w} \in \mathbb{C}^K$ is measured by

$$e_3(\Omega) = \mathbf{a}^{\mathrm{H}}(\Omega, \vartheta_0, \varphi_0)\mathbf{w} - 1 \tag{13}$$

Evaluated over a range of frequencies $\Omega \in [\Omega_l; \Omega_u]$, the overall cost function is

$$\xi_3 = \frac{1}{2\pi} \int_{\Omega_l}^{\Omega_u} |e_3(\Omega)|^2 d\Omega \ , \tag{14}$$

and the optimisation problem for the coefficients $\mathbf{w}$ can be stated as

$$\mathbf{w}_{\text{opt}} = \arg\min_{\mathbf{w}} \xi_3 \ . \tag{15}$$

The solution to (15) is given by the Wiener solution

$$\mathbf{w}_{\text{opt}} = \mathbf{R}^{-1}\mathbf{p} \tag{16}$$

with

$$\mathbf{R} = \frac{1}{2\pi} \int_{\Omega_l}^{\Omega_u} \mathbf{a}(\Omega, \vartheta_0, \varphi_0)\mathbf{a}^{\text{H}}(\Omega, \vartheta_0, \varphi_0) d\Omega$$

and

$$\mathbf{p} = \frac{1}{2\pi} \int_{\Omega_l}^{\Omega_u} \mathbf{a}(\Omega, \vartheta_0, \varphi_0) d\Omega \ .$$

This solution can be approximated by numerical integration over a specified number of frequency bins. Alternatively, we reformulate the problem as a discrete approximation over a set of $N+1$ frequencies $\Omega_n = \Omega_l + n(\Omega_u - \Omega_l)/N$, $n = 0 \ldots N$ using

$$\mathbf{e}_3 = \begin{bmatrix} e_3(\Omega_0) \\ e_3(\Omega_1) \\ \vdots \\ e_3(\Omega_N) \end{bmatrix} = \begin{bmatrix} \mathbf{a}^{\text{H}}(\Omega_0, \vartheta_0, \varphi_0) \\ \mathbf{a}^{\text{H}}(\Omega_1, \vartheta_0, \varphi_0) \\ \vdots \\ \mathbf{a}^{\text{H}}(\Omega_N, \vartheta_0, \varphi_0) \end{bmatrix} \cdot \mathbf{w} - \underline{1} = \mathbf{A}^{\text{H}}\mathbf{w} - \underline{1} \ . \tag{17}$$

This leads to $\hat{\xi}_3 = \mathbf{e}^{\text{H}}\mathbf{e}$. Differentiation w.r.t. $\mathbf{w}^*$ yields

$$\frac{\partial \hat{\xi}_3}{\partial \mathbf{w}^*} = \mathbf{A}\mathbf{A}^{\text{H}}\mathbf{w}_{\text{opt}} - \mathbf{A}\underline{1} = \underline{0} \ .$$

Therefore

$$\mathbf{w}_{\text{opt}} = (\mathbf{A}\mathbf{A}^{\text{H}})^{-1}\mathbf{A}\underline{1} = \mathbf{A}^{\dagger}\underline{1}$$

represents the desired solution.

V. Simulations and Results

Below, the architecture is simulated over one octave with $\Omega_l = \frac{\pi}{2}$ and $\Omega_u = \pi$. A total of 32 sensors are split into $M = 4$ subarrays of $K = 8$ elements each. The fractional delay filters are Hann-windowed sinc functions [9] of length $N = 25$. Noting that fractional delay filters are imperfect for $\Omega \longrightarrow \pi$, the performance at the upper limit of the frequency operating range cannot be expected to be highly accurate.

Fig. 5 shows the beamformer's directivity pattern (or gain response) $A(\vartheta, e^{j\Omega})$ for the case where the tapped delay line filters are designed appropriately as fractional delay filters for a waveform with angle of arrival of $\vartheta_o = -30°$. As a benchmark, Fig. 5 uses a steering vector for ϑ_0 and the centre frequency of the interval $[\Omega_l;\ \Omega_u]$. In contrast, Fig. 6 shows the array response for the case of narrowband filter design

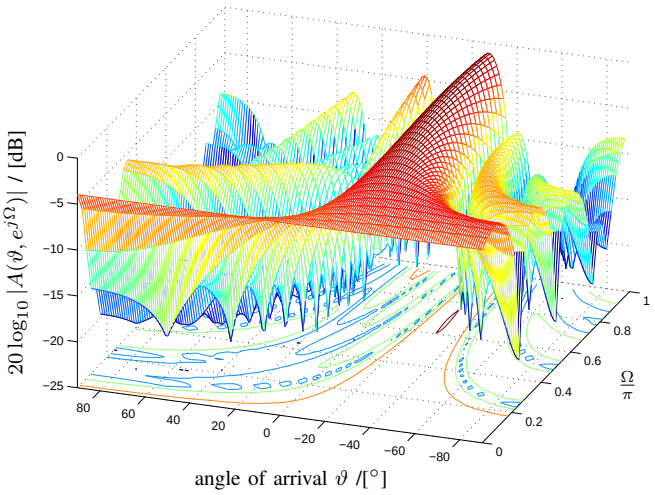

Fig. 5. Subarray architecture pointing towards $\vartheta_0 = 30°$ with narrowband beamformers selected w.r.t. centre frequency.

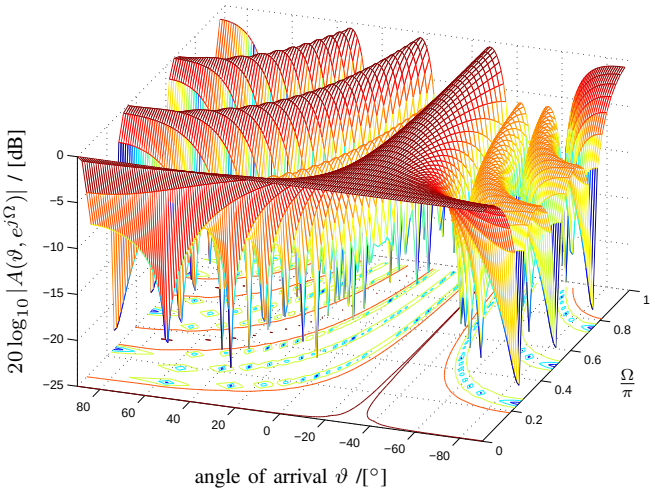

Fig. 6. Subarray architecture pointing towards $\vartheta_0 = -30°$ with narrowband beamformers optimised w.r.t. (8).

according to (16) and (17). Grating lobes have appeared, but the beam response in look direction $\vartheta_o = -30°$ better preserved than in the case of Fig. 5.

The same array configuration is used to implement a look direction of $\vartheta_0 = -60°$. In this case, the beam squinting or variation of the steering vector $\mathbf{a}(\Omega, \vartheta)$ over the operating frequency range is great for the previous example, and the narrowband beamformers introduce a greater error compared to a broadband beamformer with a tapped delay line attached to every sensor element. The result for the subarray architecture and a narrowband design at the centre frequency of the interval $[\Omega_l;\ \Omega_u]$ is shown in Fig. 7. The introduced error is such that the desired unit gain in the look direction cannot be maintained. For the proposed optimized design of the narrowband beamformer, the resulting directivity patterns are shown in Fig. 8. There is a significant difference to the standard case in Fig. 7, as the unit gain in look direction is

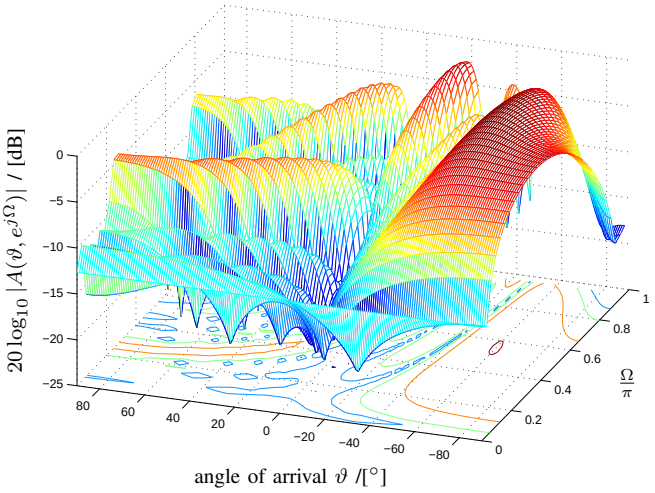

Fig. 7. Subarray architecture pointing towards $\vartheta_0 = -60°$ with narrowband beamformers selected w.r.t. centre frequency.

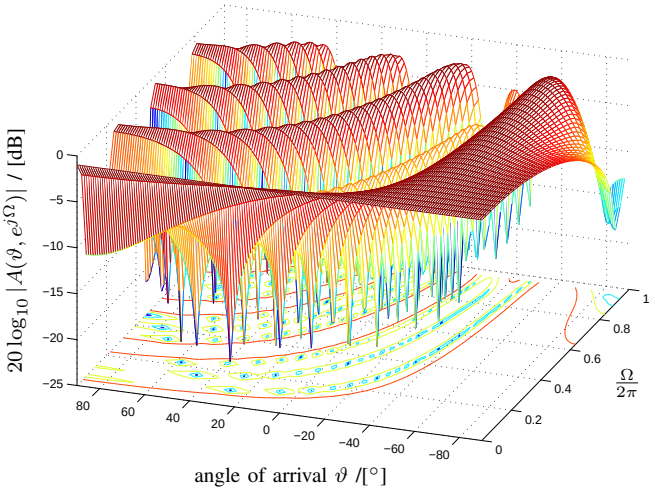

Fig. 8. Subarray architecture pointing towards $\vartheta_0 = -60°$ with narrowband beamformers optimized w.r.t. (8).

maintained. A small deviation towards $\Omega = \pi$ is due to the inaccuracies of the fractional delay filters. As a drawback of the proposed design, Figures. 6 and 8 exhibit stronger grating lobes compared to the benchmark approach in Figures. 5 and 7. A reason for this is the way the optimal design in Sec. IV tapers and therefore restricts the aperture of the array, as shown for the case of $K = 8$ coefficients for a look direction $\vartheta = -60°$ in Fig. 9. In parts, this can be bypassed by selecting non-uniform subarray configurations as discussed in [3], [4], [5]. This can be accommodated by designing, different from our architecture shown in Fig 1, the narrowband beamforming coefficients for each subarray individually.

VI. Conclusions

This paper has proposed a subarray architecture where fractional delay filters coarsely align subarrays in time. The implementation utilises windowed sinc functions of moderate

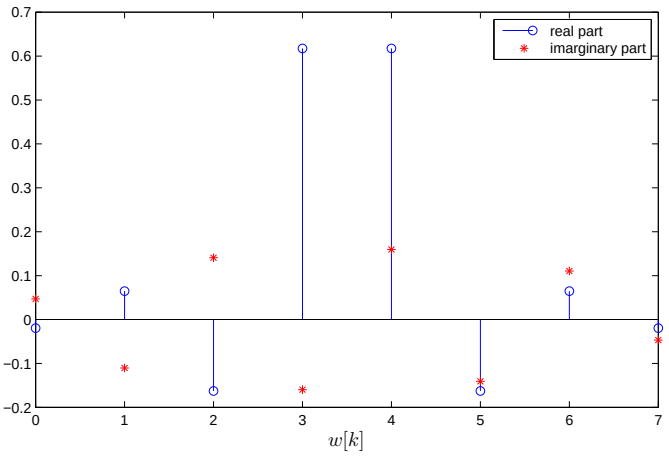

Fig. 9. Real and imaginary part of the narrowband coefficients $\mathbf{w}$ of the subarray, optimised w.r.t. broadband maintenance of the look direction $\vartheta = 60°$.

order, which can demonstrate sufficient accuracy close to up to half the sampling rate. A finer tuning for every subarray is performed by narrowband weights. If defined as phase shifts, these narrowband weights can only provide an accurate answer at one given frequency, and are likely to generate an error in the look direction gain at other frequencies.

Therefore, an error minimisation for the subarray gain deviation in look direction is required. When the designed narrowband array is operating in a wider band, the median frequency point is commonly adopted to assign the array weights. This has been shown here to generally yield suboptimal results. For the delay-and-sum beamformer, this assumption has been challenged in this paper and shown to cause higher response error at angles away from broadside direction. Instead, we have proposed a weight optimisation that can accurately impose the desired constraint, albeit at the cost of grating lobes due to a restriction of the narrowband beamformer's aperture, which is a byproduct of the optimisation procedure.

References

[1] W. Liu and S. Weiss, *Wideband Beamforming: Concepts and Techniques*, ser. Wireless Communications and Mobile Computing. Wiley, 2010.

[2] R. L. Haupt, *Timed and Phased Array Antennas*. John Wiley & Sons, Inc, 2015, pp. 1–9.

[3] ——, "Optimized weighting of uniform subarrays of unequal sizes," *Antennas and Propagation, IEEE Transactions on*, vol. 55, no. 4, pp. 1207–1210, April 2007.

[4] R. J. Mailloux, "Subarray technology for time delayed scanning arrays," in *Microwaves, Communications, Antennas and Electronics Systems, 2009. COMCAS 2009. IEEE International Conference on*, Conference Proceedings, pp. 1–6.

[5] Z.-Y. Xiong, Z.-H. Xu, S.-W. Chen, and S.-P. Xiao, "Subarray partition in array antenna based on the algorithm x," *Antennas and Wireless Propagation Letters, IEEE*, vol. 12, pp. 906–909, 2013.

[6] W.-D. Wirth, *Radar Techniques Using Array Antennas*, ser. Radar, Sonar, Navigation and Avionics. Institution of Engineering and Technology, 2013. [Online]. Available: http://digital-library.theiet.org/content/books/ra/pbra026e

[7] S. Somasundaram, "Wideband robust capon beamforming for passive sonar," *Oceanic Engineering, IEEE Journal of*, vol. 38, no. 2, pp. 308–322, April 2013.

[8] T. Laakso, V. Valimaki, M. Karjalainen, and U. Laine, "Splitting the unit delay [fir/all pass filters design]," *Signal Processing Magazine, IEEE*, vol. 13, no. 1, pp. 30–60, Jan 1996.

[9] J. Selva, "An efficient structure for the design of variable fractional delay filters based on the windowing method," *Signal Processing, IEEE Transactions on*, vol. 56, no. 8, pp. 3770–3775, Aug 2008.

[10] M. Alrmah, S. Weiss, and J. McWhirter, "Implementation of accurate broadband steering vectors for broadband angle of arrival estimation," in *Intelligent Signal Processing Conference 2013 (ISP 2013), IET*, Dec 2013, pp. 1–6.

[11] R. J. Mailloux, "Electronically scanned arrays," *Synthesis Lectures on Antennas*, vol. 2, no. 1, pp. 1–82, 2007.

[12] T. C. Q. Alfred and S. Sanyal, "Overlapped subarray architecture of an wideband phased array antenna with interference suppression capability," *Journal of Electromagnetic Analysis and Applications*, vol. 5, no. 5, pp. 201 – 204, 2013.

[13] A. B. Ben Mathews, Jacob Griesbach, "Wideband radar adaptive beamforming using frequencydomain derivative based updating."

[14] G. H. Golub and C. F. Van Loan, *Matrix Computations (3rd Ed.)*. Baltimore, MD, USA: Johns Hopkins University Press, 1996.

[15] H. Duan, B. P. Ng, C. M. S. See, and J. Fang, "Applications of the {SRV} constraint in broadband pattern synthesis," *Signal Processing*, vol. 88, no. 4, pp. 1035 – 1045, 2008.